01 Aug 2022

Superhard Single-Phase (Ti,Cr)B2 Ceramics

Lun Feng

William Fahrenholtz
Missouri University of Science and Technology, billf@mst.edu

Gregory E. Hilmas
Missouri University of Science and Technology, ghilmas@mst.edu

Laura Silvestroni

Recommended Citation

L. Feng et al., "Superhard Single-Phase (Ti,Cr)B2 Ceramics," *Journal of the American Ceramic Society*, vol. 105, no. 8, pp. 5032 - 5038, Wiley, Aug 2022.
The definitive version is available at https://doi.org/10.1111/jace.18490

Received: 8 February 2022 | Revised: 30 March 2022 | Accepted: 4 April 2022

DOI: 10.1111/jace.18490

Journal of the American Ceramic Society

RAPID COMMUNICATION

Superhard single-phase (Ti,Cr)B_2 ceramics

Lun Feng[1] | **William G. Fahrenholtz**[1] | **Gregory E. Hilmas**[1] | **Laura Silvestroni**[2]

[1]Department of Materials Science and Engineering, Missouri University of Science and Technology, Rolla, Missouri, USA

[2]CNR - ISTEC, National Research Council of Italy - Institute of Science and Technology for Ceramics, Faenza, Italy

Correspondence
Lun Feng, Department of Materials Science and Engineering, Missouri University of Science and Technology, Rolla, MO 65049, USA
Email: allen13521@gmail.com

Funding information
NATO Science for Peace and Security Program, Grant/Award Number: MYP-G5767 (SUSPENCE)

Abstract

A nominally pure and dense $(Ti_{0.9}Cr_{0.1})B_2$ ceramic was produced by spark plasma sintering of powders synthesized by boro/carbothermal reduction of oxides. The synthesized powders were a single phase and had an average particle of 0.4 ± 0.1 μm and an oxygen content of 1.2 wt%. Average Vickers hardness values of the resulting ceramics increased from 25.9 ± 0.8 GPa at a load of 9.81 N, to 46.3 ± 0.8 GPa at a load of 0.49 N. Compared to the nominally pure TiB_2 ceramic obtained under the same processing conditions, the $(Ti_{0.9}Cr_{0.1})B_2$ ceramic had higher values under the same load due to the finer average grain size (2.4 ± 1.0 μm), higher relative density, and solid solution hardening. The results indicated that the Cr addition promoted densification, suppressed grain growth, and improved the hardness of TiB_2 ceramics. This is the first report for dense and single-phase (Ti,Cr)B_2 ceramics as superhard materials.

KEYWORDS
chromium diborides, superhard materials, titanium diborides, Vickers hardness

1 | INTRODUCTION

Titanium diboride (TiB_2) ceramics have attracted wide attention as ultrahigh temperature ceramics due to their high melting point (~3230°C), hardness (~28 GPa), Young's modulus (~560 GPa), thermal conductivity (60–120 W (m K)$^{-1}$), and electrical conductivity (~10^5 S cm^{-1}) along with low theoretical density (4.52 g cm^{-3}).[1–3] These properties make TiB_2 promising for potential applications, such as ultrahigh temperature structural materials, armor, cutting tools, electrodes, and wear-resistant components.[3,4] Achieving fully dense TiB_2 is difficult due to its strong covalent bonding and low self-diffusion coefficient, which needs sintering temperatures of 1900°C and above along with the use of external pressures or long holding time up to 2 h.[5,6] However, the high sintering temperature results in significant grain growth in TiB_2 ceramics. Once the grain size becomes larger than a critical value of about 15 μm, spontaneous microcracking occurs in both grains and grain boundaries due to the stresses that develop during cooling due to the anisotropy of the thermal expansion coefficient between the a ($\alpha_a = 6.63 \times 10^{-6}$ K^{-1}) and c ($\alpha_c = 8.65 \times 10^{-6}$ K^{-1}) directions in TiB_2 grains.[5,6] In addition, the presence of surface oxides, including TiO_2 and B_2O_3, can also promote grain growth and suppress the densification of TiB_2 ceramics. These effects deteriorate the strength, hardness, and elastic constants of TiB_2 ceramics.[6]

Previous studies have reported that sintering additives, such as Al_2O_3,[4] SiC,[7,8] TiC,[9] and B_4C,[7] promoted densification at lower temperatures, improved the microstructure, and improved some mechanical properties (particularly, strength and toughness) of TiB_2 ceramics. However, most sintering additives, except B_4C, reduced the hardness of TiB_2 ceramics due to their intrinsic "softer" nature. Gu et al.[4] reported that the increase in Al_2O_3 content (0–40 vol%) resulted in an increase in relative density to 98% and fracture toughness to 6.0 MPa m$^{1/2}$, but a decrease in Vickers hardness to 21.8 GPa at a load of 196 N for TiB_2–Al_2O_3 ceramics. Yan et al.[8] reported Vickers hardness

values at a load of 196 N for fully dense TiB_2-30 vol% SiC as 18.1 GPa for SiC particles and 28.9 GPa for SiC whiskers. In contrast, Shcherbakov et al. reported that binary TiB_2–B_4C ceramics with relative densities ranging from 94% to 97% had Vickers hardness values from 37.1 to 44.8 GPa at a load of 0.98 N, whereas an equimolar mixture of TiB_2 and B_4C high energy milled with WC–Co milling media resulted in a hardness of 33 ± 3 GPa at a load of 0.49 N.[10] Neuman et al.[7] reported that a triplex ceramic containing equal volume fractions of TiB_2, SiC, and B_4C had an extremely high Vickers hardness up to ~53 GPa at a load of 0.49 N.

Our recent study reported that nominally pure, single-phase high-entropy diboride ceramics with different compositions could be produced by a two-step process.[11] Among them, $(Cr_{0.2}Hf_{0.2}Ta_{0.2}Ti_{0.2}Zr_{0.2})B_2$ ceramics had the highest relative density of 99.9%, smallest grain sizes (3.2 ± 1.3 μm), and highest Vickers hardness up to 48.3 ± 2.3 GPa. The results indicated that the presence of Cr in the solid solutions may promote densification, reduce grain size, and increase the hardness of diboride ceramics. However, single-phase $(Ti,Cr)B_2$ ceramics have not been reported to date. Previous studies indicated that the binary titanium–chromium diboride showed high hardness and good wear and oxidation resistance, although it was not clear if single-phase ceramics were formed.[12] Murthy et al. studied the effect of CrB_2 additions on the densification, properties, and oxidation resistance of TiB_2 ceramics. The solid solution between TiB_2 and CrB_2 was not complete due to the solubility limit of CrB_2 below 2000°C,[13] which resulted in low relative densities ranging from 94.0% to 96.6%.

The purpose of the present study is to investigate the densification behavior and microstructure of single-phase $(Ti,Cr)B_2$ ceramics as potential superhard materials.

2 | EXPERIMENTAL PROCEDURE

Titanium oxide (TiO_2, 99.9%, 32-nm APS; Alfa Aesar), chromium oxide (Cr_2O_3, 99.5%, 0.7 μm, Elementis, Corpus Christi, TX), and boron carbide (B_4C, purity 96.8%, 0.8 μm, HD20, H.C. Starck, Karlsruhe, Germany) were used as the starting materials. $(Ti_{0.9}Cr_{0.1})B_2$ powders were synthesized by boro/carbothermal reduction (BCTR) of the oxides with B_4C according to the stoichiometries of reactions (1) and (2). Due to the loss of B by the evaporation of B_2O_3, excess B_4C is required to ensure complete BCTR:

$$7TiO_{2(s)} + 5B_4C_{(s)} = 7TiB_{2(s)} + 5CO_{(g)} + 3B_2O_{3(g)} \quad (1)$$

$$7Cr_2O_{3(s)} + 9B_4C_{(s)} = 12CrB_{2(s)} + 9CO_{(g)} + 4B_2O_{3(g)} \quad (2)$$

Oxides and 13 wt% excess B_4C were mixed by ball-milling for 4 h using yttria-stabilized ZrO_2 media with acetone as the solvent. The slurries were dried by rotary evaporation at 60°C and passed through a 150-mesh sieve. To improve particle contact, promote reaction, and suppress loss of powder during processing, powder mixtures were pressed into disks with a diameter of 25 mm under a uniaxial pressure of 2 MPa. The BCTR reaction was performed at 1650°C for 2 h in a resistance-heated graphite element furnace (Model 3060, Thermal Technology, Santa Rosa, CA) under vacuum (~13.3 Pa). The reacted products were gently crushed and collected.

The as-synthesized $(Ti_{0.9}Cr_{0.1})B_2$ powders were loaded in a graphite die (inner diameter: 20 mm) lined with graphite foil and densified at 2000°C for 10 min under mild vacuum (~2 Pa) and a uniaxial pressure of 50 MPa by spark plasma sintering (SPS, DCS10, Thermal Technology, Santa Rosa, CA). To improve the purity of the $(Ti_{0.9}Cr_{0.1})B_2$ ceramic and to promote densification, a two-step sintering was performed.[11,14] In the first step, powders were heated at 100°C min^{-1} under mild vacuum (~2 Pa) and a uniaxial load of 15 MPa up to 1650°C where the temperature was held for 5 min to promote reaction and removal of residual oxides. In the second stage, the uniaxial pressure was increased to 50 MPa within 1 min after holding at 1650°C, and the furnace was then heated at 150°C min^{-1} to the final densification temperature of 2000°C. After isothermal holding at the final temperatures for 10 min, the furnace cooled to 1000°C at 100°C min^{-1} and under a uniaxial pressure of 25 MPa and then allowed to cool naturally to room temperature. The temperature was measured by an optical pyrometer focused on a hole that was drilled to a depth of half the thickness of the graphite die body. Shrinkage curves were recorded and then corrected by adjusting the total ram displacement to compensate for the thermal expansion of the graphite die, which was done by recording dimensional changes for an empty graphite die heated using the same sintering profile as the powders. For comparison, nominally pure TiB_2 powder was synthesized and densified using the same processes.

Phase compositions were analyzed by an X-ray diffraction (XRD, PANalytical X-Pert Pro, Malvern Panalytical Ltd., Royston, United Kingdom) method. Powders were examined in the as-synthesized state. Sintered specimens were ground on both sides to remove the graphite foil and any reaction layers prior to further analysis. Bulk densities were measured by Archimedes' method using distilled water as the immersing medium.

Theoretical densities (ρ_{th}) were calculated using the following equation:

$$(\rho_{th}) = (n \bullet M) / (N \bullet V) \quad (3)$$

where n and M are the number of atoms and the molecular weight in one-unit cell, N is Avogadro's number, and V

is the lattice volume. M was calculated based on an ideal composition of $(Ti_{0.9}Cr_{0.1})B_2$, whereas V was calculated using the lattice parameters that were determined by analyzing XRD patterns of dense billets using Rietveld refinement (RIQAS software, MDI, Livermore, CA). The morphologies and particle sizes of the synthesized powders were analyzed using scanning electron microscopy (SEM, Raith eLine Plus, Dortmund, Germany). Microstructures, grain sizes, and metal distributions of sintered specimens were examined using SEM with energy-dispersive spectroscopy (EDS, BRUKER). Specimen surfaces were polished to a 0.25-μm finish using successively finer diamond suspensions. A computer-based image analysis program (ImageJ, National Institutes of Health, Bethesda, MD) was used to estimate the sizes of particles and grains. At least 300 grains per specimen were measured to determine average particle and grain sizes. The oxygen contents of synthesized powders and sintered ceramics were analyzed by the inert gas fusion method (TC500, LECO, St. Joseph, MI). The sintered samples were pulverized prior to the measurement, and a standard specimen was first measured for calibration. The oxygen content of the standard sample is measured with a precision of $\pm$0.008 wt%.

Microhardness was measured by Vickers indentation following ASTM C1327 (Model Duramin 5, Struers Inc., Cleveland, OH), under indentation loads of 0.49, 0.98, 1.96, 4.90, and 9.81 N for a dwell time of 15 s. Reported values are the average of 10 valid measurements. To minimize the error in testing below 4.90 N, indentation sizes were measured using a 3D digital optical microscope (HiROX, HIROX-USA, Hackensack, NJ). Young's and shear moduli were measured using a dynamic elastic properties analyzer by an ultrasonic method (DEPA, Jagdish Electronics, Bangalore, India). Fracture toughness was determined using the direct crack measurement method described by Anstis et al.[15] Indents were made on a polished surface using a 98.1 N load for 15 s. The reported values were the average of six indentations.

3 | RESULTS AND DISCUSSION

XRD patterns of the synthesized $(Ti_{0.9}Cr_{0.1})B_2$ powders showed that nominally pure and single-phase diboride with a hexagonal structure were observed after BCTR at 1650°C, as shown in Figure 1. No oxide phases were detected by XRD, and the oxygen content was 1.2 wt%. The results indicated that the BCTR reaction was almost complete after heating at 1650°C, which was attributed to the fine particle size of the starting powders, 32 nm and 0.7 μm, and the reduced onset temperature for the reaction under vacuum.[16] Nominally pure TiB_2 powder was also synthesized after BCTR at 1650°C, based on its XRD pattern

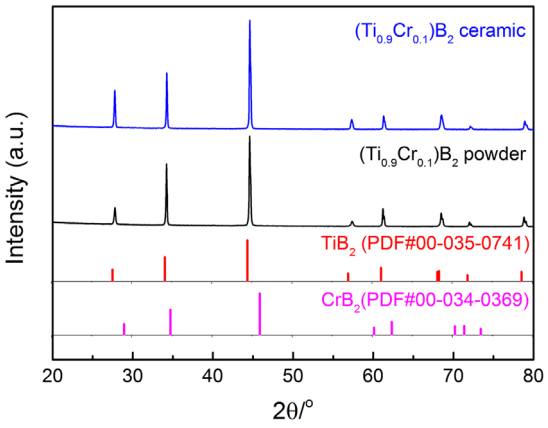

FIGURE 1 XRD patterns of $(Ti_{0.9}Cr_{0.1})B_2$ powders synthesized by BCTR at 1650°C and $(Ti_{0.9}Cr_{0.1})B_2$ ceramics produced by SPS at 2000°C. BCTR, boro/carbothermal reduction; XRD, X-ray diffraction

(not shown), with measured lattice parameters reported in Table 1. The lattice parameters for $(Ti_{0.9}Cr_{0.1})B_2$ powder were smaller than those for TiB_2 powder, which indicated that Cr had dissolved into the TiB_2 lattice due to the smaller lattice parameters of CrB_2, as shown in Table 1. In addition, XRD analysis indicated that the solid solution between TiB_2 and CrB_2 was nearly complete at temperatures as low as 1650°C, although previous studies and the phase diagram showed that the complete solid solution between TiB_2 and CrB_2 across the entire composition range required temperatures above 2000°C.[13] In the present study, the higher degree of formation of solid solution was achieved at lower temperature presumably due to the finer particle size of the synthesized boride powders and the lower Cr content. The average particle size of the synthesized TiB_2 and $(Ti_{0.9}Cr_{0.1})B_2$ powders was similar, around 0.4 μm, as shown in Figure 2A,C.

After SPS at 2000°C, single-phase $(Ti_{0.9}Cr_{0.1})B_2$ with no residual impurity phases was detected by XRD, as shown in Figure 1. The lattice parameters for the $(Ti_{0.9}Cr_{0.1})B_2$ ceramic were smaller than those measured for the $(Ti_{0.9}Cr_{0.1})B_2$ powder, which indicated that the preparation of solid solution was complete after densification. The sintered $(Ti_{0.9}Cr_{0.1})B_2$ ceramic had also much lower oxygen content, 0.01 wt%, than that of as-synthesized powders (1.20 wt%), due to the removal of surface oxides during densification.[14]

After heating to 1650°C, solid solution formation between TiB_2 and CrB_2 was nearly complete based on the following observations:

(1) $(Ti_{0.9}Cr_{0.1})B_2$ powder had a single phase with a hexagonal structure.
(2) The lattice parameters of $(Ti_{0.9}Cr_{0.1})B_2$ powder were close to those of the sintered $(Ti_{0.9}Cr_{0.1})B_2$ ceramic.

TABLE 1 Compositions, synthesis temperatures, lattice parameters, and average particle/grain sizes of TiB_2 powders, $(Ti_{0.9}Cr_{0.1})B_2$ powders, and $(Ti_{0.9}Cr_{0.1})B_2$ ceramics

Compositions	Synthesis temperature (°C)	Lattice parameters (nm)			Average crystallite size (μm)	Ref.
		a	*c*	*c/a*		
TiB_2 powder	1650	0.3030	0.3229	1.066	0.4 ± 0.1	Present study
$(Ti_{0.9}Cr_{0.1})B_2$ powder	1650	0.3026	0.3211	1.061	0.4 ± 0.1	
$(Ti_{0.9}Cr_{0.1})B_2$ ceramic	2000	0.3022	0.3213	1.063	2.4 ± 1.0	
TiB_2	–	0.3030	0.3229	1.066	–	#00-035-0741
CrB_2	–	0.2973	0.3071	1.033	–	#00-034-0369

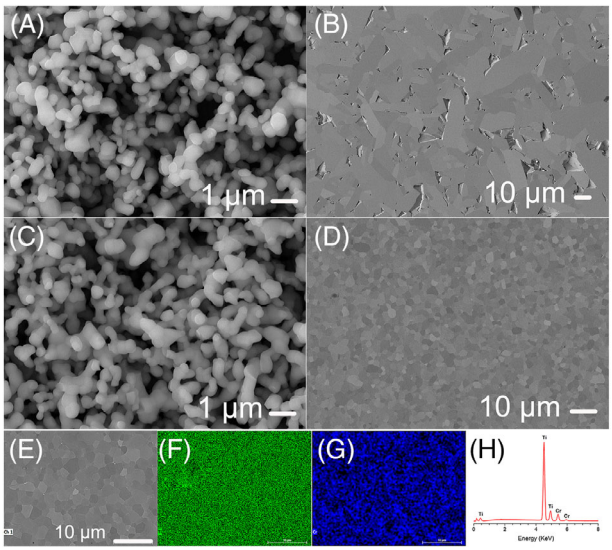

FIGURE 2 SEM micrographs of (A) TiB_2 powder, (B) TiB_2 ceramic, (C) $(Ti_{0.9}Cr_{0.1})B_2$ powder, and (D) $(Ti_{0.9}Cr_{0.1})B_2$ ceramic, along with the corresponding (E, F (Ti), G (Cr)) EDS maps and (H) EDS spectrum of the $(Ti_{0.9}Cr_{0.1})B_2$ ceramic. EDS, energy dispersive spectroscopy; SEM, scanning electron microscopy

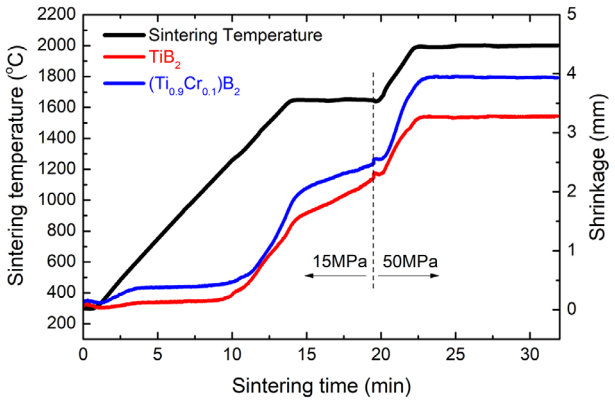

FIGURE 3 Shrinkage curves as a function of sintering time for TiB_2 and $(Ti_{0.9}Cr_{0.1})B_2$ ceramics during SPS at 2000°C. SPS, spark plasma sintering

(3) The sintered $(Ti_{0.9}Cr_{0.1})B_2$ ceramic displayed a single phase by XRD and with similar lattice parameters between experimental values and those calculated ($a = 0.3024$ nm and $c = 0.3214$ nm) using Vegard's law and the reported lattice parameters of TiB_2 and CrB_2.

For comparison, signs of incomplete solid solution reactions would be (1) multiple phases in XRD patterns; (2) significantly different lattice parameters between powder and sintered materials; or (3) discrepancies between calculated and experimental lattice parameters.

An almost fully dense $(Ti_{0.9}Cr_{0.1})B_2$ ceramic was produced by SPS at 2000°C. The relative density was 99.6% for $(Ti_{0.9}Cr_{0.1})B_2$, which was higher than the relative density of 97.9% achieved for pure TiB_2, as shown in Table 2 and Figure 2B,D. These results indicated that Cr promoted the densification of TiB_2 ceramics. A previous study reported that TiB_2–CrB_2 ceramics produced by hot pressing at 1750°C had relative densities ranging from 94.0% to 96.6%.[13] Compared to previous results, higher relative densities were achieved in the present study.

Densification curves were similar for $(Ti_{0.9}Cr_{0.1})B_2$ and nominally pure TiB_2 ceramics during the SPS process, as shown in Figure 3. Below about 1250°C, little shrinkage occurred, presumably due to particle rearrangement under the low uniaxial pressure of 15 MPa. Significant shrinkage was observed from about 1250 to 1650°C. During the isothermal hold at 1650°C, continuous shrinkage was observed for both compositions, which indicates that densification was not complete. A sharp increase in shrinkage occurred after the isothermal hold at 1650°C due to the application of a higher uniaxial pressure of 50 MPa. Subsequently, distinct shrinkage was observed for the $(Ti_{0.9}Cr_{0.1})B_2$ ceramics during heating, but shrinkage stopped at the beginning of the isothermal hold at 2000°C. Slight expansion was observed through the entire isothermal hold, which indicates that densification reached completion. In contrast, distinct shrinkage with a slower rate was observed for the pure TiB_2 ceramics below 2000°C, whereas continuous shrinkage occurred through

TABLE 2 Compositions, sintering conditions, theoretical density (ρ_{th}), relative density (ρ), Vickers hardness (HV0.1), Young's modulus (E), shear modulus (G), fracture toughness (K_{Ic}), and average grain size (mgs) of TiB_2 and $(Ti_{0.9}Cr_{0.1})B_2$ ceramics compared with previous studies

Compositions	Sintering ($^\circ C\,MPa^{-1}\,min^{-1}$)	ρ_{th} ($g\,cm^{-3}$)	ρ (%)	HV0.1 (GPa)	E (GPa)	G (GPa)	K_{Ic} ($MPa\,m^{1/2}$)	mgs (μm)	Ref.
TiB_2	SPS/2000/50/10	4.48	97.9	36.7 ± 4.3	454 ± 6	204 ± 3	–	27.5 ± 23.1	Present study
$(Ti_{0.9}Cr_{0.1})B_2$		4.57	99.6	35.3 ± 4.2	558 ± 8	247 ± 3	2.2 ± 0.2	2.4 ± 1.0	
TiB_2–2.5 wt%CrB_2	HP/1750/35/60	–	96.6	23.9 ± 1.3	–	–	2.8 ± 0.1	–	13
TiB_2–5.0 wt%CrB_2		–	94.8	23.7 ± 2.0	–	–	4.3 ± 0.4	–	
TiB_2–10.0 wt%CrB_2		–	94.0	23.9 ± 1.1	–	–	5.0 ± 1.0	2–4	

Abbreviation: HP, hot pressing.

the entire isothermal hold at 2000°C, which indicates that densification of pure TiB_2 was not fully complete. More shrinkage was observed for $(Ti_{0.9}Cr_{0.1})B_2$ ceramics compared to the nominally pure TiB_2 ceramic, considering also the slope of the curves, which was consistent with the higher measured relative density of the $(Ti_{0.9}Cr_{0.1})B_2$ ceramic, as shown in Table 2. In comparison to a previous study,[13] the present results indicated that Cr additions promoted the densification of TiB_2 ceramics presumably due to a change in densification kinetics caused by the solid solution effect.[17,18]

The synthesized TiB_2 and $(Ti_{0.9}Cr_{0.1})B_2$ powders had similar particle sizes of about 0.4 ± 0.1 μm, as shown in Figure 2A,C. The fine particle size of the starting powder mixtures and mild vacuum promoted BCTR at lower temperatures, thus resulting in fine particle size after BCTR[16]. Neck formation between particles was presumed to be due to the formation of B_2O_3 during synthesis, as previously observed during boride synthesis.[19] However, the pure TiB_2 ceramics had an average grain size of about 27 ± 23 μm after SPS at 2000°C. In addition, microcracks, particle pull-out, and residual porosity were also observed, as shown in Figure 2B. The microstructure of the pure TiB_2 ceramic produced in the present study was consistent with the results reported in previous studies.[5,6] The high sintering temperature resulted in strong grain growth, thus inducing microcracks due to anisotropy of the thermal expansion coefficient between the a and c axes of TiB_2. Particle pull-out occurred during the polishing step because of microcracks after sintering. In contrast, the $(Ti_{0.9}Cr_{0.1})B_2$ ceramic exhibited a denser and finer microstructure without the formation of microcracks, as shown in Figure 2D. The average grain size was 2.4 ± 1.0 μm, which was much smaller than that of the pure TiB_2 ceramic. The corresponding EDS maps (Figure 2E–G) and spectrum (Figure 2H) of $(Ti_{0.9}Cr_{0.1})B_2$ ceramic show that Ti and Cr were uniformly distributed in the scanned area, which was consistent with the single phase detected by XRD. The results indicate that the Cr addition promoted densification and suppressed the grain growth of TiB_2 grains, which was consistent with the measured relative densities and densification behavior.

In the present study, CrB_2 was introduced to TiB_2 by in situ reaction. Solid solution formation inhibited the motion of grain boundaries, thus suppressing the grain growth during sintering. Fine grain has high surface energy, which can provide high driving force for sintering. Therefore, the introduction of Cr into TiB_2 lattice promoted densification and suppressed grain growth.

The mechanical properties of TiB_2 and $(Ti_{0.9}Cr_{0.1})B_2$ ceramics are summarized in Table 2. The Young modulus of $(Ti_{0.9}Cr_{0.1})B_2$ was 558 ± 8 GPa, which was higher than the value (528 GPa) predicted using a volumetric rule of mixture calculation based on the nominal compositions and using the reported modulus values for TiB_2 (~560 GPa)[3] and CrB_2 (210 GPa).[20] The higher Young modulus could be due to the solid solution effect. In contrast, the pure TiB_2 ceramic had a lower modulus value due to the lower relative density and microcracks. The fracture toughness of the $(Ti_{0.9}Cr_{0.1})B_2$ ceramic produced in the present study was 2.2 ± 0.2 MPa $m^{1/2}$, which was lower than the values for TiB_2–CrB_2 ceramics reported in a previous study, possibly due to the different CrB_2 contents and uncomplete solid solution in the previous study.[13]

Figure 4 shows the Vickers hardness as a function of indentation load for TiB_2 and $(Ti_{0.9}Cr_{0.1})B_2$ ceramics compared with previous studies. The hardness was 25.9 ± 0.8 GPa at a load of 9.81 N, and it increased to 46.3 ± 0.8 GPa at a load of 0.49 N. Hardness values increased as the indentation load decreased due to the indentation size effect. At a load of 0.98 N, the $(Ti_{0.9}Cr_{0.1})B_2$ ceramic in the present study had much higher hardness (35.3 ± 4.2 GPa) than (Ti,Cr)B_2 ceramics (around 23.9 GPa), reported in a previous study, due to the higher relative density, finer grain size, and complete solid solution achieved in the present study.[13] At a load of 0.49 N, the hardness value for $(Ti_{0.9}Cr_{0.1})B_2$ was slightly higher than that of TiB_2, which indicated that the Cr addition increased the hardness of TiB_2. In addition, the $(Ti_{0.9}Cr_{0.1})B_2$ ceramic exhibited hardness values that were

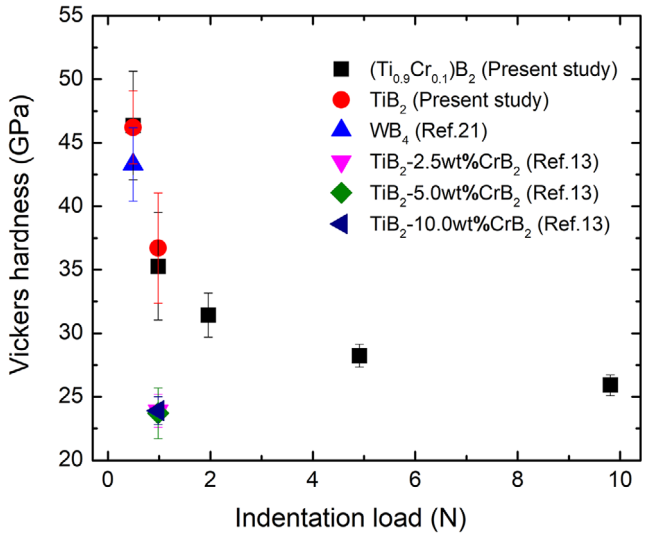

FIGURE 4 Vickers hardness as a function of indentation load for TiB_2 and $(Ti_{0.9}Cr_{0.1})B_2$ ceramics compared to (Ti,Cr)B_2 and WB_4 ceramics from other studies[13,21]

higher than or comparable to superhard materials, such as nominally pure WB_4 (43.3 ± 2.9 GPa)[21] and other TMB_4 (TM = W, Re, Mo, Ta, Os, and Tc; 40–54 GPa) ceramics.[22] The results indicated that solid solution hardening was able to produce superhard TiB_2-based materials.

4 | CONCLUSIONS

To summarize, a nominally pure, dense, and single-phase $(Ti_{0.9}Cr_{0.1})B_2$ ceramic was produced by SPS at 2000°C using powders synthesized by BCTR. Nearly complete solid solution occurred already upon synthesis at 1650°C. The synthesized $(Ti_{0.9}Cr_{0.1})B_2$ powders had an average particle size of 0.4 ± 0.1 μm and oxygen content of 1.2 wt%. The sintered $(Ti_{0.9}Cr_{0.1})B_2$ ceramic had a hardness of 46.3 ± 0.8 GPa that was higher than a nominally pure TiB_2 ceramic at a load of 0.49 N, due to the finer average grain size (2.4 ± 1.0 μm), higher relative density, and solid solution hardening.

These results indicate that 0.1 at% Cr substitution within TiB_2 lattice promoted densification, suppressed grain growth, and improved the hardness of TiB_2 ceramics. This study demonstrated a reliable way to widen the application fields of TiB_2 ceramics by synthesis and sintering in milder conditions without jeopardizing the mechanical properties.

ACKNOWLEDGMENTS

This research was sponsored by the NATO Science for Peace and Security Program under Grant Number: MYP-G5767 (SUSPENCE).

ORCID

Lun Feng https://orcid.org/0000-0002-6895-9950
William G. Fahrenholtz https://orcid.org/0000-0002-8497-0092
Laura Silvestroni https://orcid.org/0000-0003-4595-0299

REFERENCES

1. Wuchina EJ, Opila E, Opeka MM, Fahrenholtz WG, Talmy IG. UHTCs: ultra-high temperature ceramic materials for extreme environment applications. Interface. 2007;16:30–6.
2. Tell R, Sigl LS, Takagi K.Boride-based hard materials. In: Riedel R, editor. Handbook of ceramic hard materials. Weinheim: Wiley-VCH; 2000:802–945.
3. Basu B, Raju GB, Suri AK. Processing and properties of monolithic TiB_2 based materials. Int Mater Rev. 2006;51:352–74.
4. Gu ML, Huang CZ, Xiao SR, Liu HL. Improvement in mechanical properties of TiB_2 ceramics tool materials by the dispersion of Al_2O_3 particles. Mater Sci Eng A2018;486:167–70.
5. Sulima I, Figiel P, Susniak M, Swiatek M. Sintering of TiB_2 ceramics. Mater Sci Eng2007;28:687–90.
6. Wang WM, Fu ZY, Wang H, Yuan RZ. Influence of hot pressing sintering temperature and time on microstructure and mechanical properties of TiB_2 ceramics. J Eur Ceram Soc. 2002;22:1045–9.
7. Neuman EW, Brown-Shaklee HJ, Hilmas GE, Fahrenholtz WG. Titanium diboride–silicon carbide–boron carbide ceramics with super-high hardness and strength. J Am Ceram Soc.2018;101:497–501.
8. Yan SR, Foong LK, Lyu ZJ. Technical performance of co-addition of SiC particulates and SiC whiskers in hot pressed TiB_2-based ultrahigh temperature ceramics. Ceram Int. 2020;46:19443–51.
9. Ismail AE, Alimin AJ, Mohd Tobi AL, Khalid A, Abdullah HZ, Masood I, et al. Fabrication of TiB_2–TiC composites optimized by different amount of carbon in the initial Ti-B-C powder mixture. Appl Mech Mater. 2013;315:720–3.
10. Silvestroni L, Failla S, Gilli N, Melandri C, Savaci, Turan S, Sciti D. Disclosing small scale length properties in core-shell structured B_4C–TiB_2 composites. Mater Des. 2021; 197:109204.
11. Feng L, Monteverde F, Fahrenholtz WG, Hilmas GE. Superhard high-entropy AlB_2-type diboride ceramics. Scr Mater. 2021;199:113855.
12. Samsonov GV, Markovskii LYa, Zhigach AF, Valyashko MG. Boron and its compounds and alloys [in Russian], Kiev: Izd-vo. AN USSR; 1960.
13. Murthy TSRCh, Sonber JK, Subramanian C, Fotedar RK, Gonal MR, Suri AK. Effect of CrB_2 addition on densification, properties and oxidation resistance of TiB_2. Int J Refract Hard Met. 2009;27:976–84.
14. Feng L, Fahrenholtz WG, Hilmas GE. Processing of dense high-entropy boride ceramics. J Eur Ceram Soc. 2020;40:3815–23.
15. Anstis GR, Chantikul P, Lawn BR, Marshall DB. A critical evaluation of indentation techniques for measuring fracture toughness: I, direct crack measurements. J Am Ceram Soc. 1981;64:533.
16. Feng L, Fahrenholtz WG, Hilmas GE. Two-step synthesis process for high-entropy diboride powders. J Am Ceram Soc. 2020;103:724–30.
17. Wang HL, Lee SH, Feng L. The processing and properties of (Zr, Hf)B_2-SiC nanostructured composites. J Eur Ceram Soc. 2014;34:4105–9.

18. Grigoriev O, Neshpor I, Vedel D, Mosina T, Silvestroni L. Influence of chromium boride on the oxidation resistance of ZrB_2-$MoSi_2$ and ZrB_2-SiC ceramics. J Eur Ceram Soc. 2021;41:2207–14.
19. Wang HL, Lee SH, Kim HD. Nano-hafnium diboride powders synthesized using a spark plasma sintering apparatus. J Am Ceram Soc. 2012;95:1493–6.
20. Bauccio ML. ASM engineered materials reference book. United States of America: ASM International; 1994.
21. Mohammadi R, Lech AT, Xie M, Weaver BE, Yeung MT, Tolbert SH, et al. Tungsten tetraboride, an inexpensive superhard material. Proc Natl Acad Sci USA. 2011;108:10958–62.
22. Wang M, Li YW, Cui T, Ma YM, Zou GT. Origin of hardness in WB_4 and its implications for ReB_4, $Ta B_4$, MoB_4, TcB_4 and OsB_4. Appl Phys Lett. 2018;93:101905.

How to cite this article: Feng L, Fahrenholtz WG, Hilmas GE, Silvestroni L. Superhard single-phase $(Ti,Cr)B_2$ ceramics. J Am Ceram Soc. 2022;105:5032–5038.
https://doi.org/10.1111/jace.18490